

# Identification of $\lambda$ Bootis stars using IUE spectra

## II. High resolution data

E. Solano<sup>1</sup> and E. Paunzen<sup>2</sup>

<sup>1</sup> INSA-LAEFF, P.O. Box 50727, E-28080 Madrid, Spain (esm@vilspa.esa.es)

<sup>2</sup> Institut für Astronomie der Universität Wien, Türkenschanzstrasse 17, A-1180 Wien, Austria (Ernst.Paunzen@univie.ac.at)

Received 15 March 1999 / Accepted 28 June 1999

**Abstract.** Stars included in the catalogue of  $\lambda$  Bootis stars by Paunzen et al. (1997) with high resolution spectra (FWHM: 0.10–0.25 Å) in the INES Archive of the International Ultraviolet Explorer satellite (IUE) are analyzed here in order to establish membership criteria for the  $\lambda$  Bootis group. Line-ratios of carbon to heavier elements (Si, Al, Ca) were adopted as criteria in the SWP range (1150–1980 Å). For the LWP range (1850–3350 Å), the intensity of metallic lines (Fe and Mg) was used. These criteria, together with those derived for low resolution spectra, make the IUE Final Archive a powerful tool to find new  $\lambda$  Bootis candidates.

**Key words:** stars: chemically peculiar – stars: early-type – ultraviolet: stars

### 1. Introduction

Since the peculiarity of  $\lambda$  Bootis itself was firstly discovered by Morgan et al. (1943) different criteria have been proposed over the years to define and characterize the  $\lambda$  Bootis stars as a class. Unfortunately, most of these criteria are not unique to the  $\lambda$  Bootis but they are also shared by other groups (e.g. Ap, helium-weak and horizontal branch stars). This has led to a certain confusion and it is not difficult to find in the literature stars that are catalogued as  $\lambda$  Bootis by some authors but not classified as such by others. Reviews on this topic can be found in Paunzen (1998) and Gerbaldi & Faraggiana (1993). Recently, Paunzen et al. (1997) has catalogued  $\lambda$  Bootis stars as Population I, metal-poor (except of C,N,O and S) A to F-type stars and this is the definition adopted in this paper.

As stated in Solano & Paunzen (1998, Paper I hereafter), one of the main reasons of the reduced number of well established members of the  $\lambda$  Bootis class is the lack of features in the optical range suitable as discriminating criteria. This problem can be alleviated if the ultraviolet range is used. In Paper I we demonstrated that it is possible to find features in the low resolution IUE spectra that can be taken as unambiguous membership criteria for the  $\lambda$  Bootis group. In this paper a similar analysis using high resolution spectra is performed.

**Table 1.**  $\lambda$  Bootis stars included in Paunzen et al. (1997) with IUE high resolution observations

Identification	$T_{\text{eff}}$	log g	IUE images		
			LWP	LWR	SWP
HD 31295	8775	4.15	02098	14125	17885
			02557		17886
HD 38545	8100	3.6	31516		55979
HD 105058	7800	3.65	11967		
HD 110411	8850	4.2		07658	08909
					43603
					43604
HD 111786	7500	4.0	02561		21945
			03557		23243
					43606
HD 125162	8500	4.1	02099	14116	17873
				14117	17874
					42081
HD 141851	8150	3.85	02560		
HD 142703	7200	3.95			48197
HD 170680	9700	4.1	08223		28341
HD 183324	8700	4.1	08220		28338
					28342
HD 192640	7900	3.9	02100	14127	17888
HD 221756	8600	3.85	02559		43131
					21944

### 2. Analysis

$\lambda$  Bootis stars included in Paunzen et al. (1997) with available high resolution spectra (FWHM: 0.10–0.25 Å, depending on camera and order number) of any of the three operational cameras (SWP: 1150–1980 Å; LWP/LWR: 1850–3350 Å) have been analyzed (Table 1). The spectra have been retrieved from the INES database<sup>1</sup>. INES (IUE Newly Extracted Spectra) is a project developed at VILSPA defined as the final step in the archive and distribution phase of the IUE data. The INES high resolution spectra are derived from the Final Archive files but they are presented as concatenated spectra. The order concatenation has been defined in such a way that the signal-to-noise

Send offprint requests to: E. Solano (esm@vilspa.esa.es)

<sup>1</sup> <http://ines.vilspa.esa.es>

**Table 2.** Same as Table 1 but for the standard stars

Identification	$T_{\text{eff}}$	$\log g$	[Fe/H]	IUE images		
	This work/Sources	This work/Sources	Sources	LWP	LWR	SWP
HD 18331	8150	3.5	-0.39(1)	26810		49327
HD 26015	6850/6850(2)	4.3	+0.30(2)	17033		
				17476		
HD 26911	6800/6860(2)	4.3	+0.27(2)		08869	
HD 56537	8275	3.75	-0.04(1)	07916		46982
				27876		50525
HD 58946	6950/6974(3),7020(4)	4.1/4.11(3),4.0(4)	-0.31(4)	24951		46983
HD 71155	9950/9910(5)	4.1	+0.00(16)	26668		49061
HD 87696	8000/8160(6)	4.1/4.6(6)	-0.02(1)	12055		
				28367		
HD 97603	8250/8080(7),8270(8)	3.8/3.9(6)	-0.02(1)	09585		31085
				10896		31086
						46745
HD 97633	9250/9460(14),9450(15)	3.8/3.45(14),3.7(15)	+0.43(14),-0.12(15)		02901	03291
					02902	03292
					11981	15505
					15932	19972
					15933	19973
					15934	19974
					15935	19975
					15946	19987
					16103	20169
					16113	20170
					16114	20178
					16115	20179
						20180
HD 102647	8660/8857(9),8850(7)	4.2/4.0(9),4.05(10)	-0.40(1)	07414		30994
				10926		31108
				21946		31117
						33340
						43327
HD 116842	8150/7971(11),8230(6)	4.0	-0.06(1)	10149	11712	
				10366		
				23050		
HD 128167	6700/6650(12),6763(11)	4.35/4.3(12),4.4(11)	-0.39(12),-0.40(11)		05316	
HD 130109	10000/10110(5),9820(6)	3.75	-0.40(1)	07492	01922	33631
				13307		33632
HD 134083	6600/6617(11)	4.4/4.5(11)	+0.10(11)	19658	16011	
HD 198001	9200/9470 (13)	3.6/3.64(13)	+0.07(13)	25700		50599

*References:* **1:** Smalley (1993a); **2:** Boesgaard & Budge (1988); **3:** Smalley & Kupka (1997); **4:** Alonso et al. (1996); **5:** Sokolov (1995); **6:** Malagnini & Morossi (1990); **7:** Napiwotzki et al. (1993); **8:** Smalley (1993b); **9:** Malagnini & Morossi (1997); **10:** Smalley & Dworetzky (1995); **11:** Blackwell & Lynas-Gray (1994); **12:** Boesgaard et al. (1998); **13:** Hill (1995); **14:** Rentzsch-Holm (1997); **15:** Hill & Landstreet (1993); **16:** Eggen (1987)

ratio of the overlapping region is maximized, avoiding the highly noisy order edges where the ripple correction may be less efficient. INES flux values are the same as the Final Archive values but a velocity correction has been applied to the wavelength scale to convert the data in both wavelength ranges and both apertures into an internally consistent wavelength scale. Furthermore, the derived errors are provided in absolute flux units which is not the case in the Final Archive files.

The  $\lambda$  Bootis spectra were compared to those of stars included in the refined list of MK standards given by Jascheck

& Gómez (1998) (“standards”, hereafter; Table 2). Spectra of Field Horizontal Branch (FHB, hereafter) stars were also analyzed (Table 3). Effective temperatures and surface gravities of the  $\lambda$  Bootis and standard stars were derived using Moon & Dworetzky (1985) whereas an average of the most recent values in the literature was adopted for the FHB stars. A detailed description of the method can be found in Paper I.

**Table 3.** Same as Table 1 but for field Horizontal-Branch stars

Identification	$T_{\text{eff}}$	log g	IUE images		
			LWP	LWR	SWP
HD 109995	8300(1),	3.15(1),	03625	02899	23288
HD 109995	8350(2)	3.36(2)			
			03626	05343	23289
			03662	08051	23294
			03667		23358
			06319		23365
			06348		25180
			06349		26333
					26348
					26368
HD 128801	10250(3)	3.4(3)	18148		
			18335		
HD 161817	7500(1),	2.95(1),		06280	
HD 161817	7580(2)	3.0(2)			

*References:* **1:** de Boer et al. (1997); **2:** Hayes & Philip (1988); **3:** Adelman & Philip (1994)

### 3. Results

#### 3.1. Feature selection

Quoting Baschek & Searle (1969) "...  $\lambda$  Bootis stars can be defined as stars whose composition resembles that of  $\lambda$  Boo itself...". Although the UV range is rich in spectral lines from a variety of chemical elements, the typically high rotational velocities of  $\lambda$  Bootis stars lead to blending features preventing from using most of the lines. The feature selection have been done on the basis of the definition of the  $\lambda$  Bootis class (metal-poor stars except for C, N, O and S, Fig 1) and they have been named according to the main contributor as identified from the computation of the synthetic spectrum generated using ATLAS9 (Kurucz 1993) (Table 4). Weak and strongly blended features which cannot be accurately measured were discarded. This is the reason why some lines of elements potentially of interest according to the  $\lambda$  Bootis definition have not been taken into account (e.g. N I 1493 Å, N I 1495 Å, N I 1743 Å, N I 1745 Å, S I 1820 Å). Also, two lines selected in Paper I are not considered here: C I 1931 Å, lying outside of the photometrically corrected region in high dispersion spectra and the feature at  $\lambda$  1741 Å due to its limited performance compared to the new features present in high dispersion spectra (Si II 1526 Å, Ca II 1839 Å)

In Figs. 2,3 the equivalent widths of these features have been plotted as a function of the effective temperature for the  $\lambda$  Bootis, FHB and the standard stars. Equivalent widths were measured as described in Paper I and only for those features not affected by any external error sources (saturation, cosmic rays, bright spots, reseau marks). If more than one spectrum is available for a given star, the average equivalent width and the standard deviation (which gives an estimation of the internal error of the measurements) were calculated. It is important to stress that the equivalent width is defined as the area enclosed by the feature and a pseudo-continuum drawn through its highest points. Therefore, as stated in Paper I, these "pseudo-equivalent widths"

**Table 4.** Selected features

Camera	Identification	Components	Wavelength Range (1)	
SWP	Si II 1526.71 Å		1525.63-1528.08	
		C I 1657	1654.47-1660.62	
		C I 1656.27 Å		
		C I 1656.93 Å		
		C I 1657.01 Å		
		C I 1657.38 Å		
		C I 1657.91 Å		
		C I 1658.12 Å		
		Al II 1670.79 Å		1669.04-1672.56
		Ca II 1839		1837.46-1839.35
LWP		Ca II 1838.01 Å		
		Ca II 1840.06 Å		
	Fe II 2599		2597.56-2602.58	
		Fe II 2597.94 Å		
		Fe II 2598.37 Å		
		Fe II 2599.40 Å		
		Fe II 2599.47 Å		
		Fe II 2600.42 Å		
	Fe II 2632		2630.15-2634.86	
		Fe II 2630.07 Å		
	Fe II 2631.01 Å			
	Fe II 2631.32 Å			
	Fe II 2631.61 Å			
Mg II 2800		2786.32-2809.10		
	Mg II 2795.53 Å			
	Mg II 2802.70 Å			
Mg I 2852.13 Å		2851.33-2855.09		

(1) Wavelength range used for the measurement of the equivalent widths of the features.

will be useful only for an empirical classification but not for a detailed abundance analysis. As reported in Paper I there is a correlation between equivalent width and effective temperature. Variations in EW due to surface gravity and abundance variations from star to star are negligible when compared to the intrinsic measurement errors.

#### 3.2. Ratio between absorption lines

According to the definition of the  $\lambda$  Bootis class, the differences between  $\lambda$  Bootis and standard as well as FHB stars can be enhanced by using line-ratios of elements with solar abundance to the heavier elements instead of using equivalent widths of single lines. Fig. 4 shows the derived line-ratios for the SWP range. We consider, therefore, a star to be a member of the  $\lambda$  Bootis group if:

- C I 1657 / Si II 1527 > 3
- C I 1657 / Al II 1670 > 3
- C I 1657 / Ca II 1839 > 8

Note that in Paper I we derived the criterion C I 1657 / Al II 1670 > 2 for the low resolution spectra. This difference is due to the fact that the equivalent width

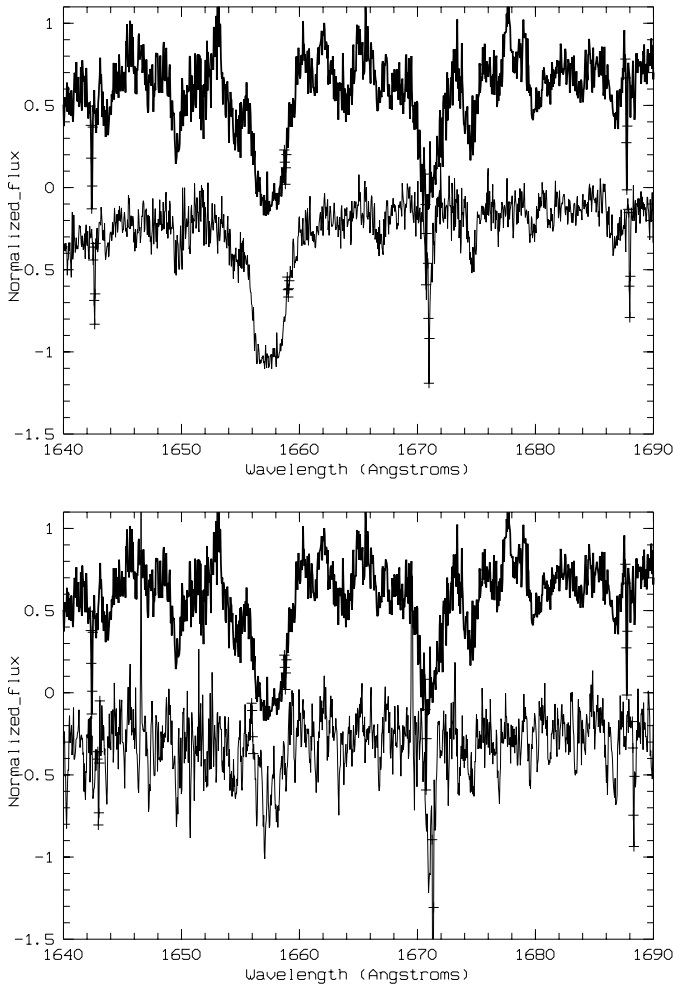


**Fig. 1.** Comparison between a typical spectrum of a standard star (HD 102647, thick line) and a)  $\lambda$  Bootis star (HD 183324) (top); b) Field horizontal branch star (HD 109995) (bottom). For clarity, the  $\lambda$  Bootis and FHB spectra have been shifted down

measurements of the high resolution spectra are much more accurate leading to a tighter equivalent width – temperature relation and, therefore, a more accurate line-ratio based criterion. This can be easily seen comparing Fig. 2 of this paper to Fig. 2 of Paper I. Also note that the number of criteria is different from Paper I which is due to the different number of features selected for low and high resolution spectra: a higher number of features decreases the probability of misclassification associated to errors in the equivalent widths and also permits classification even if some parts of the spectra are useless (e.g. saturation). This is why high resolution spectra are always preferred for the identification of  $\lambda$  Bootis candidates. Nevertheless, despite its greater accuracy, high resolution spectra represent only one third of the INES Archive which makes necessary, in some cases, to use the low resolution criteria although they may be less significant.

Unfortunately, there are no representative lines of elements with solar abundance (i.e. carbon, oxygen, nitrogen, sulphur) in the LWP range. Therefore, although clearly separated from the

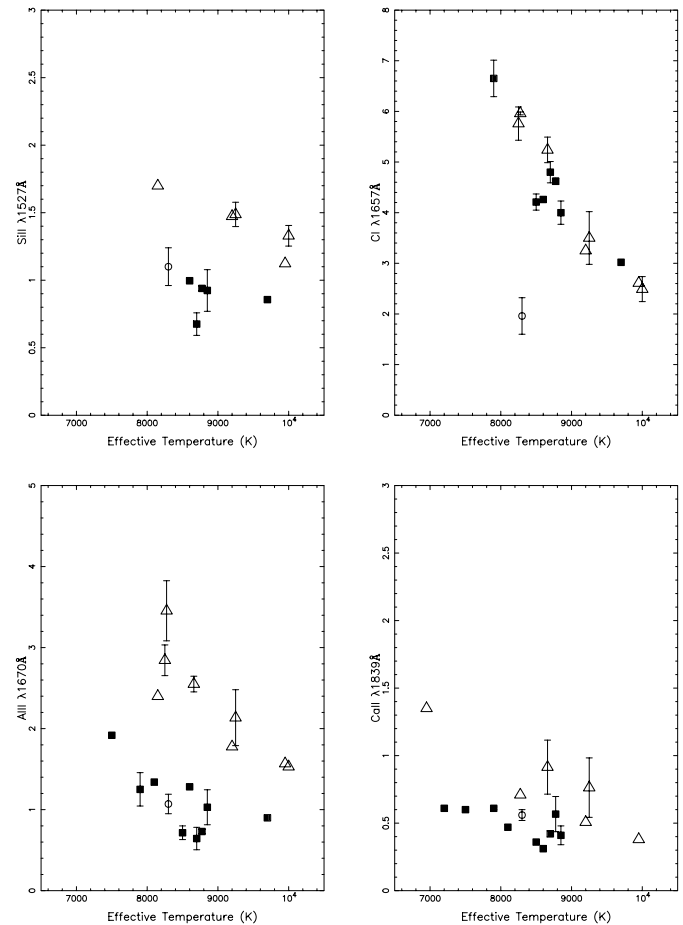


**Fig. 2.** Equivalent widths (in  $\text{\AA}$ ) of the absorption features quoted in Table 4 for  $\lambda$  Bootis (squares), field horizontal branch (circles) and standard stars (triangles) (SWP range). Error bars represent the standard deviation in the measurements of equivalent widths if more than one spectrum is available for a given star

standards,  $\lambda$  Bootis cannot be distinguished from FHB or other metal-poor stars in this range (Fig. 3). Moreover, it is not possible to define a criterion valid for the entire range of  $T_{\text{eff}}$ . Accordingly, the selection criteria in the LWP range has been defined as following:

$$EW(2599 \text{ \AA}) < 2.5 - 1.7 \times (T_{\text{eff}} - 6500)/4000$$

$$EW(2632 \text{ \AA}) < 2 - (T_{\text{eff}} - 6500)/5000$$

$$EW(2800 \text{ \AA}) < 13 - (T_{\text{eff}} - 6500)/500$$

$$EW(2852 \text{ \AA}) < 1.5 - 1.5 \times (T_{\text{eff}} - 6500)/3500$$

where  $T_{\text{eff}}$  is the effective temperature of the star. Taking the above given limits one is able to find metal-poor (Fe and Mg) stars in the relevant temperature domain. Further astrophysical information (e.g. spectroscopical analysis) is then necessary to define the true nature of a candidate star.

#### 4. Conclusions

We have analyzed IUE high resolution spectra of  $\lambda$  Bootis stars from Paunzen et al. (1997) as well as FHB and standard stars.

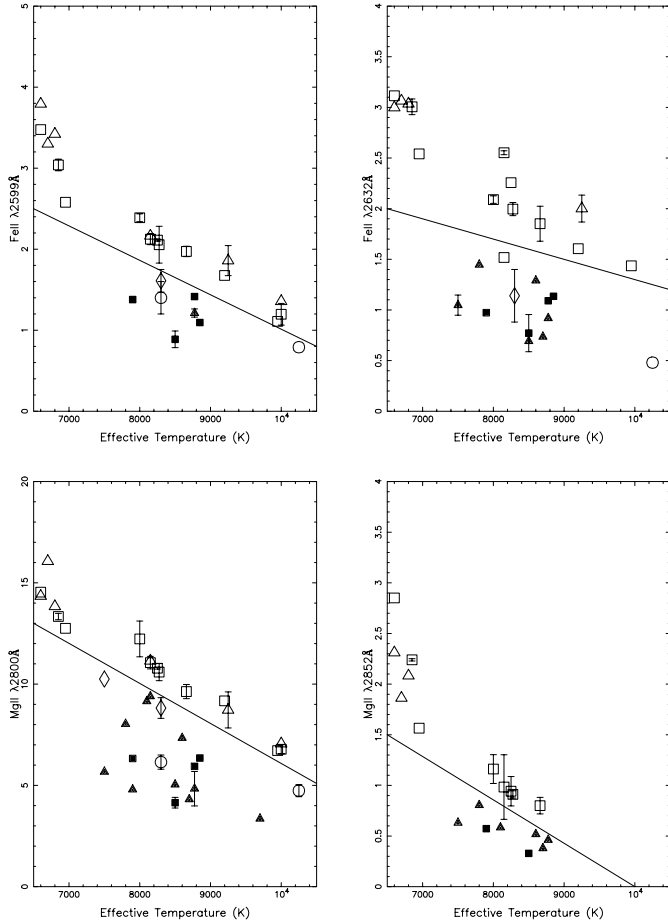


**Fig. 3.** Same as Fig. 2 but for the LWP/LWR range. Squares and triangles represent standard stars (LWP, LWR cameras respectively), filled squares and filled triangles represent  $\lambda$  Bootis stars (LWP, LWR respectively) and circles and diamonds represent FHB stars (LWP, LWR respectively)

Easily identifiable and unambiguous indicators of the  $\lambda$  Bootis phenomenon in the ultraviolet have been identified in the SWP range of high resolution spectra: we consider a star to be member of the  $\lambda$  Bootis group if:

- C I 1657 / Si II 1527 > 3
- C I 1657 / Al II 1670 > 3
- C I 1657 / Ca II 1839 > 8

These line-ratio based criteria are independent of the effective temperature and evolutionary status. For the LWP range, criteria to differentiate between  $\lambda$  Bootis and standard stars have been defined. On the basis of these criteria, as well as those derived for low resolution spectra, a search of  $\lambda$  Bootis candidates is being presently carried out using the INES database and the results will be part of a subsequent paper.

*Acknowledgements.* EP acknowledges support from the Fonds zur Förderung der wissenschaftlichen Forschung (FWF), project S7303-AST; *Asteroseismology-AMS*. Based on INES data from the IUE satellite.

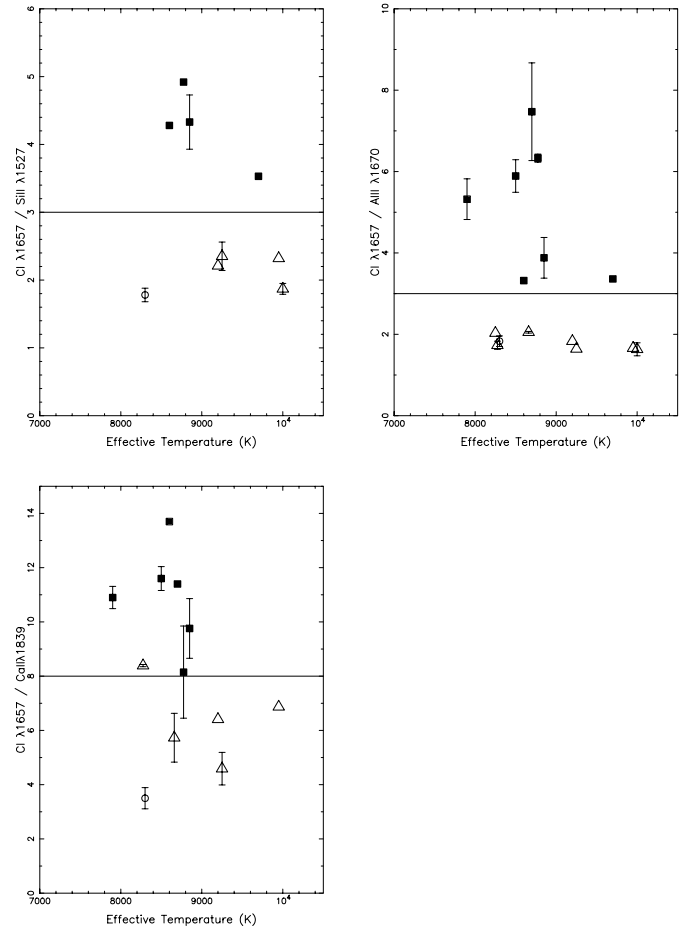


**Fig. 4.** Same as Fig. 2 but for the line-ratios

## References

- Adelman S.J., Philip A.G.D., 1994, MNRAS 269, 579  
 Alonso A., Arribas S., Martínez-Roger C., 1996, A&AS 117, 227  
 Baschek B., Searle L., 1969, ApJ 155, 537  
 Blackwell D.E., Lynas-Gray A.E., 1994, A&A 282, 899  
 Boesgaard A.M., Budge K.G., 1988, ApJ 332, 410  
 Boesgaard A.M., Deliyannis C.P., Stephens A., Lambert D.L., 1998, ApJ 492, 727  
 de Boer K.S., Tucholke H.J., Schmidt J.H.K., 1997, A&A 317, L23  
 Eggen O.J., 1987, AJ 93, 393  
 Gerbaldi M., Faraggiana R., 1993, PASPC 44, 368  
 Hayes D.S., Philip A.G.D., 1988, PASP 100, 801  
 Hill G.M., 1995, A&A 294, 536  
 Hill G.M., Landstreet J.D., 1993, A&A 276, 142  
 Jaschek C., Gómez A.E., 1998, A&A 330, 619  
 Kurucz R.L., 1993, CD-ROM 1–23, Smithsonian Astrophysical Observatory  
 Malagnini M.L., Morossi C., 1990, A&AS 85, 1015  
 Malagnini M.L., Morossi C., 1997, A&A 326, 736  
 Moon T.T., Dworetzky M.M., 1985, MNRAS 217, 305  
 Morgan W.W., Keenan P.C., Kellman E., 1943, Atlas of Stellar Spectra. Univ. Chicago Press, Chicago  
 Napiwotzki R., Schönberner D., Wenske V., 1993, A&A 268, 653  
 Paunzen E., Weiss W.W., Heiter U., North P., 1997, A&AS 123, 93  
 Paunzen E., 1998, Contrib. Astron. Obs. Skalnaté Pleso 27, 395  
 Rentzsch-Holm I., 1997, A&A 317, 178

Smalley B., 1993a, A&A 274, 391

Smalley B., 1993b, MNRAS 265, 1035

Smalley B., Dworetsky M.M., 1995, A&A 293, 446

Smalley B., Kupka F., 1997, A&A 328, 349

Sokolov N.A., 1995, A&AS 110, 553

Solano E., Paunzen E., 1998, A&A 331, 633 (Paper I)